

Combustion Dynamic Analysis of Gas Turbine Engine

M.V.H.Satish Kumar,

Associate Professor, Department of Mechanical Engineering
PVP Siddhartha Institute of Technology, Kanuru, Vijayawada – 7.
Andhra Pradesh, India.

Abstract The need for better fuel efficiency and less exhaust emissions has prompted rapid advancement in today's gas turbine engines. These innovations require more accurate condition monitoring systems to achieve optimal gas turbine performance. Burning a leaner flame reduces NOx emissions but may increase instability (combustion dynamics) at the same time. Combustion Instability can damage components in the combustion chamber such as nozzles, baskets, transition pieces and downstream components such as blades, resulting in downtime and loss of revenue.

The aim of this Project is to analyse the behaviour of a backward-facing step non-premixed combustor using Computational tools & compare the results with experimental data already available. Different parameters affecting the various stages & aspects of combustion process such as unsteady heat release, incomplete combustion, noise generation, interaction between flame, flow field & acoustics are intensively studied.

In this Project, combustion process of methane & air in a Backward Facing Step Combustor was examined using ANSYS Fluent Package for the acoustic excitation. 3-component velocity measured downstream of the inlet was used to determine the spatial average of turbulent intensity. The instantaneous and average velocity fields for both cold and combusting flows have been obtained using CFD package FLUENT.

1. Introduction

The need for better fuel efficiency and less exhaust emissions has prompted rapid advancement in today's gas turbine engines. These innovations require more accurate condition monitoring systems to achieve optimal gas turbine performance. Burning a leaner flame reduces NOx emissions but may increase instability (combustion dynamics) at the same time. Combustion Instability can damage components in the combustion chamber such as nozzles, baskets, transition pieces and downstream components such as blades, resulting in downtime and loss of revenue.

1.1 COMBUSTION INSTABILITY: BACKGROUND

Flames possess intrinsic instabilities associated with the combustion process itself & could become unstable also in response to superimposed oscillations, among which pressure oscillations are the most common. The unsteady coupling between pressure oscillations and the flame leads to unstable combustion. This is the phenomenon of combustion instability. The suppression of this coupling is the essential mission of the control problem. The strong coupling between pressure oscillations and the dynamics of unsteady heat release from flames arises in the following way. When a fluid element is heated during the combustion process, its expansion produces an initially weak pressure wave that radiates into the surrounding region. This pressure wave could get reflected from the boundary of the combustion system, and return to affect the flame surface slightly. This time-dependent effect results in a time-dependent volume change in fluid element in the combustion zone, and serves as a source of a new pressure disturbance. If the new disturbance is in phase with the old, a sustained feedback mechanism could lead to large amplitudes of pressure oscillations. Large pressure oscillations limit the operating range of a combustion system by adversely affecting the stability and survival of the flame. They also produce intense vibrations, structural damage, and high burn rates. They may propagate upstream from the combustion zone and affect the composition of the fuel-air mixture; cause a change in the atomization and vaporization process in a system using liquid fuel; organize the unstable mode in the shear layer feeding the combustion zone; produce organized concentrated vortices through its interaction with geometrical discontinuities in the system, etc.

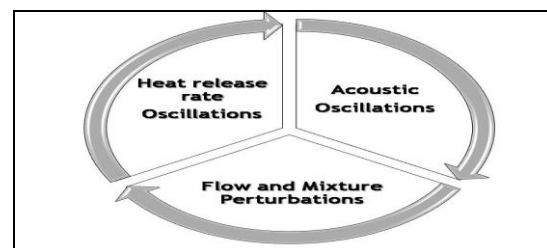


Fig. 1.1 Schematic of the feedback process responsible for combustion instability (Bernier et al., 2004).

1.2 NON-PREMIXED BACKWARD FACING STEP COMBUSTOR: A gas turbine combustor configuration is as shown in the fig. below. It's a confined complex geometry with or without swirl & a sudden expansion.

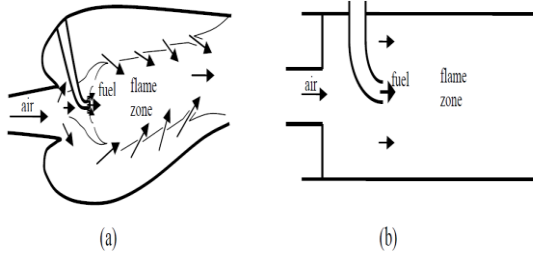


Fig. 1.2 Schematic of (a) a typical gas turbine combustor and (b) simplified geometry.

A backward-facing step combustion chamber is an example of a wall-bounded flow. It involves reattachment of separated turbulent shear layers and is an established benchmark in Computational Fluid Dynamics (CFD).

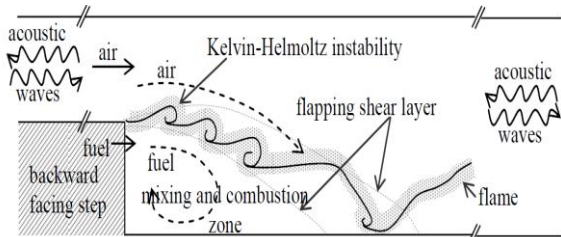


Fig. 1.3 Schematic description of flow field-flame-acoustic interaction process in a backward-facing step non-premixed combustor (Chakravarthy et al., 2007).

With this experiment the behavior of the turbulence models near walls can be validated in general. Moreover, during the intake stroke the air flows through the intake duct via the runners and valves in the combustion chamber. This is roughly comparable with the geometry of the BFS experiment and therefore a representative benchmark for the simulation.

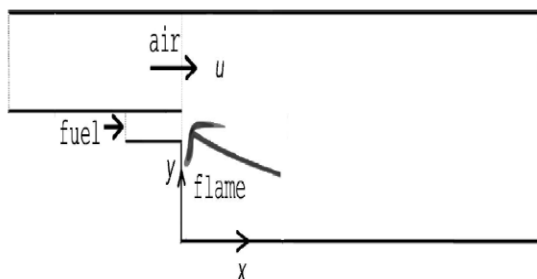


Fig: 1.4 Schematic description of a BFS

1.3 IMPORTANT PARAMETERS:

Acoustic characteristics are strongly influenced by two important non-dimensional quantities, namely Helmholtz and Strouhal numbers. The Helmholtz number is defined as

$$He = \frac{fL}{c}$$

Where, f = the dominant frequency, and c = velocity of sound according to reference condition,

Constancy of the Helmholtz number would signify that the observed dominant frequency corresponds to the natural acoustic mode of the duct, although not necessarily with any ideal acoustic boundary conditions.

The Strouhal number is defined as

$$St = \frac{fh}{U}$$

Where, U is the spatio-temporal mean air-flow velocity at the inlet.

A constant value of the Strouhal number would indicate that the observed dominant frequency corresponds to that due to any vortex shedding process or shear layer oscillation in the flow field, referred to a vortex shedding mode.

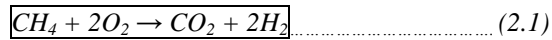
2. THEORETICAL CONSIDERATIONS:

2.1 Combustion Basics

For the majority of fuels, the available energy is stored within the chemical bonds of the fuel molecules. This chemical energy contained in the fuel can be extracted in several different ways. The most common method of extracting this energy is through combustion. During combustion, the chemically energetic molecules of the fuel are rapidly oxidized, typically with oxygen in air, to form more stable combustion products while producing large amounts of energy in the form of heat (Moran and Shapiro, 2004).

The combustion process itself is relatively complex. It is an interaction of fluid dynamics, thermodynamics, chemical kinetics and heat transfer all occurring simultaneously. One simple model to represent the combustion process is an overall stoichiometric equation, which shows a single

reaction transforming the reactant species into the product species. An example stoichiometric combustion equation can be seen below for the hydrocarbon fuel methane.



In reality, the single step reaction depicted in Equation 2-1 does not exist. Instead, numerous different reactions occur in rapid succession, producing and consuming intermediate molecules (Glassman and Yetter, 2008). Ultimately, the products shown in Equation 2.1 are the chief products of the combustion process. Since the overall thermodynamics of process does not depend significantly on the intermediate molecules, overall stoichiometric equations are useful in studying thermodynamic properties of fuels (Glassman and Yetter, 2008).

A useful way to classify the mixture ratio of fuel and oxidant is through the equivalence ratio. The equivalence ratio is the ratio of the actual fuel-oxidant ratio to the stoichiometric fuel-oxidant ratio (Moran and Shapiro, 2004). The stoichiometric fuel oxidant ratio is the mixture of fuel and oxidant that results in complete combustion of the fuel with no leftover oxidant or fuel, as depicted in Equation 2.1. Mathematically, the equivalence ratio is defined as

$$\boxed{\phi = (F/O) / (F/O)_{st}} \dots\dots\dots (2.2)$$

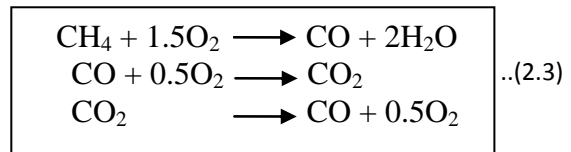
Where, ϕ is the equivalence ratio, F/O represents the ratio of fuel to oxidant, and the subscript st denotes the stoichiometric conditions. When equivalence ratio is less than one, then the fuel-oxidant mixture is said to be lean; hence there is excess oxidizer. When the equivalence ratio is greater than one, the fuel-oxidant mixture is said to be rich; hence there is excess fuel.

As was mentioned earlier, air is commonly used as the oxidant in combustion. Air mostly consists of oxygen and nitrogen, along with carbon dioxide, argon, water vapour, and other trace elements.

The numerous reaction steps that occur in a combustion process are important in determining certain characteristics of combustion. Examples include how quickly a combustion progresses from the reactants to products and the formation of pollutants (Glassman and Yetter, 2008). This is a field of study known as chemical kinetics. In general, the reaction steps in combustion are chain reactions and can be placed into four categories: chain initiation, chain branching, chain propagation, and chain termination.

In chain initiation, the fuel molecule reacts to form radicals. Chain branching steps produce more radicals while chain propagation steps maintain the same number of radicals. A chain termination step destroys radicals (Kuo, 2005; Feldick, 2007). All of these reaction steps occur at various points in a combustion process and have a hand in determining the overall characteristics of the combustion.

In this study, the fuel used is methane (CH_4) and is injected from the step corner of the backward facing step combustor. The chemical reactions involved in this combustion can be expressed as 3-step chemistry, shown below



The theory involved in non-premixed combustion in the backward facing step combustion chamber is, in the non-premixed combustion, the fuel and oxidizer enter the reaction zone in distinct streams. This is in contrast to premixed systems, in which reactants are mixed at the molecular level before burning. Examples of non-premixed combustion include pulverized coal furnaces, diesel internal-combustion engines and pool fires. Under certain assumptions, the thermo chemistry can be reduced to a single parameter. The mixture fraction, denoted by f , is the mass fraction that originated from the fuel stream. In other words, it is the local mass fraction of burnt and un-burnt fuel stream elements (C, H, etc.) in all the species (CO_2 , H_2O , O_2 , etc.).

The approach is elegant because atomic elements are conserved in chemical reactions. In turn, the mixture fraction is a conserved scalar quantity, and therefore its governing transport equation does not have a source term. Combustion is simplified to a mixing problem, and the difficulties associated with closing non-linear mean reaction rates are avoided. Once mixed, the chemistry can be modelled as being in chemical equilibrium with the Equilibrium model, being near chemical equilibrium with the Steady Laminar Flame let model, or significantly departing from chemical equilibrium with the Unsteady Laminar Flame let model.

2.2 Non-Premixed Combustion

Non-premixed modelling involves the solution of transport equations for one or two conserved scalars (the mixture fractions). Equations for individual species are not solved. Instead, species concentrations are derived from the predicted mixture fraction fields. The thermo

chemistry calculations are pre-processed and then tabulated for look-up in FLUENT. Interaction of turbulence and chemistry is accounted for with an assumed-shape Probability Density Function (PDF).

3. NUMERICAL SIMULATION METHODOLOGY:

3.1 Computational Model

To solve the governing equations of chemical kinetics and fluid dynamics, the software package FLUENT was utilized due to its ability to couple chemical kinetics and fluid dynamics. FLUENT is a computational fluid dynamics commercial software program that is used throughout the research and industrial communities. At its heart, FLUENT is a numerical solver.

In computational fluid dynamics, the differential equations that govern the problem are discretized into finite volumes and then solved using algebraic approximations of differential equations. These numerical approximations of the solution are then iterated until adequate flow convergence is reached. FLUENT is also capable of importing kinetic mechanisms and solving the equations governing chemical kinetics. The chemical kinetics information is then coupled into fluid dynamics equations to allow both phenomena to be incorporated into a single problem.

Since, FLUENT is a packaged software package, it comes with certain limitations. As was mentioned earlier, the current version of FLUENT is limited to kinetics mechanisms with 500 reactions and 50 chemical species. This precludes many mechanisms, such as those in Curran et al. (2002) and Smith et al. (2010). There are many options to specify when setting up a computational fluid dynamics model. The options used in this work are presented in Table 3.1

Solver type	Pressure based
Viscous model	Reynolds Stress (7 eq.)
Gravitational effects	Off
Pressure-velocity coupling	SIMPLE
Momentum equation discretization	Third-order MUSCL
Species Equations Discretization	Third-order MUSCL
Energy equation discretization	Third-order MUSCL
Turbulent Kinetic Energy	Second order upwind
Turbulent dissipation rate	Third-order MUSCL
Reynolds stresses	Third-order MUSCL
Transient formulation	First order implicit

Table: 3.1 Computational Model

As was explained previously, the work studied was at unsteady-state, so time effects were taken into account. The viscous model was set to RSM because this work is focused only on turbulent combustion phenomena. With this in mind, the Reynold's number of the unburned gases needed to be kept above 13000 to ensure turbulent flow. As mentioned earlier, gravitational effects were not considered in order to eliminate unnecessary variables in analyzing the results.

The SIMPLE method of velocity-coupling was used in which the mass conservation solution is used to obtain the pressure field at each flow iteration (Anderson, 1995). The numerical approximations for momentum, energy, and species transport equations were all set to third order MUSCL. In order to properly justify using these schemes, it was necessary to show that the grid used in this work had adequate resolution to accurately capture the physics occurring within the domain. In other words, the results needed to be independent of the grid resolution. This was verified by running simulations with higher resolution grids, as will be explained later.

Overall, the computational model solved the following flow equations: mass continuity, r momentum, x momentum, energy and n-1 species conservation equations where, n is the number of species in the reaction. The nth species was determined by the simple fact that the summation of mass fractions in the system must equal one.

3.1.1 Physical Model Description

A diagram of the physical model used in the tests for this research can be seen in Figure 3.1

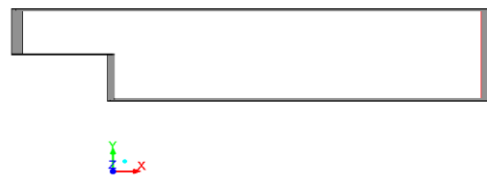


Fig: 3.1 Physical model used in testing.

As can be seen in Figure 3.1, the physical model was backward facing step combustor with a step length of 30mm and air inlet also being 30 mm, and width being 60 mm. Air flow moves from left to right. The fuel (Methane CH₄) is injected from the step corner near the air flow.

Left end of the chamber was set as inlet with a uniform velocity normal to the boundary 9.42 m/s. The right end of the chamber was set as an atmospheric pressure outlet. The walls were set as

adiabatic with zero flux of both mass and chemical species.

3.1.2 Finite Volume Mesh

The physical model seen in Figure 3.1 was given a finite volume mesh to use in the computational simulations. After some trial and error, it was determined that the simulations were most stable with a very fine mesh near the corner of the step (element length taken as 0.5 mm) where the fuel is injected and interacts with air.

Also, it was determined that the chemical reactions occurred within the initial length of the chamber after the step. With this in mind, it was decided to employ a fine hexahedral mesh in the initial length of the chamber. In this fine mesh region, the mesh was made even finer near the wall to allow for the proper processing of the boundary layer effects. The rest of the chamber was provided with a mesh merely allowed for proper development of the combustion product flow before the atmospheric pressure outlet.

This section of the model was given a relatively coarse hexahedral mesh. The size of the resulting mesh is summarized in the Table 3.2 below.

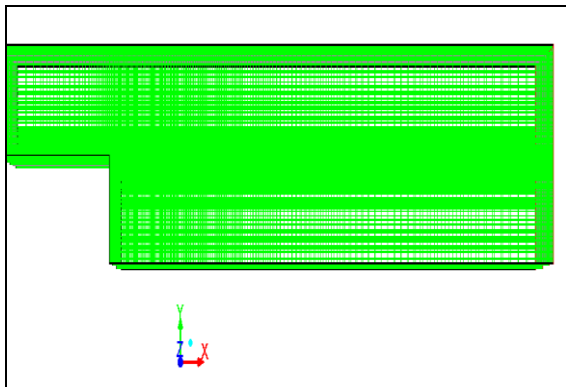


Fig:3.2 X-Y Plane cross-sectional view

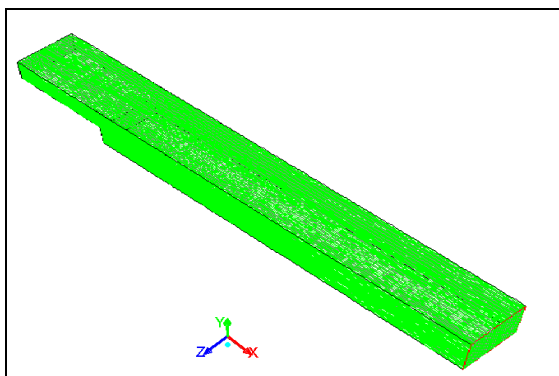


Fig: 3.3 The 3-D view of the geometry

Approximate number of nodes is around 8 lakhs.

3.2 Problem Description

A. Inlet Condition		B. Outlet Condition	
Mass flow air inlet	0.0204 kg/s	Pressure Outlet	1 atm
Mass flow fuel inlet	0.000142 kg/s		

Table: 3.2 Mass flow boundary conditions

Wall boundary condition	Adiabatic Wall
Reynolds Number	18000
Turbulence Intensity	5%
Hydraulic Diameter	0.04

Table: 3.3 Boundary condition

In the model setup for this work, the wall was given an adiabatic condition. That means that all of the heat produced by the combustion process must be contained within the tube and moved downstream to the outlet.

4. Results Discussions and Conclusion

4.1 Simulation results of temperature, species, velocity, reaction rate and turbulence intensities contours are shown below.

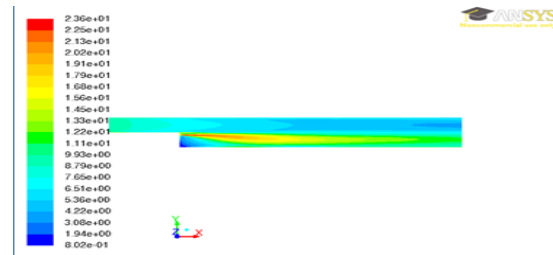


Fig. 4.1 Contours of Turbulent Intensity

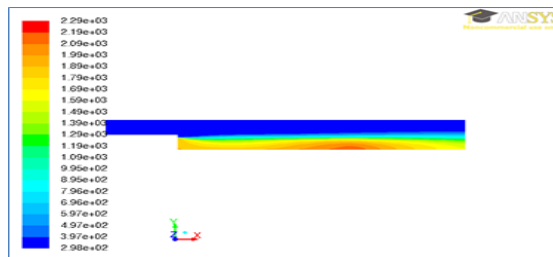


Fig. 4.2 Contours of Static Temperature

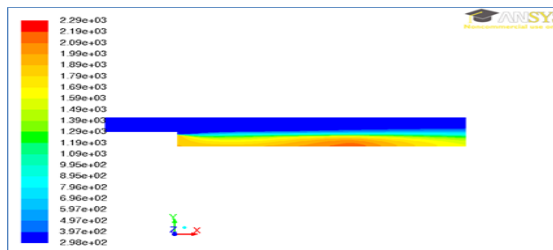


Fig. 4.3 Contours of Total Temperature

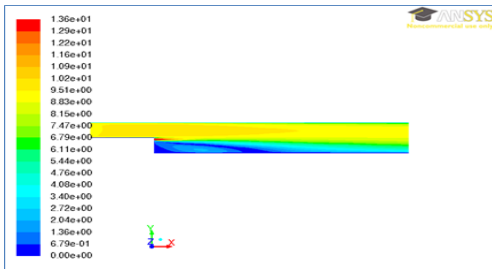


Fig. 4.4 Contours of Velocity Magnitude

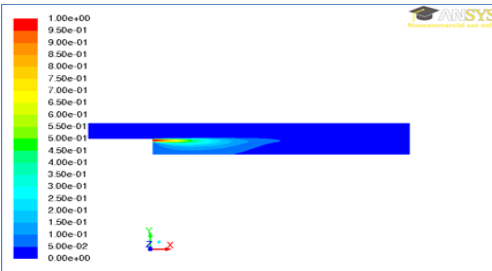


Fig. 4.5 Contours of Mass Fraction of CH_4



Fig. 4.6 Contours of Rate of Reaction-1

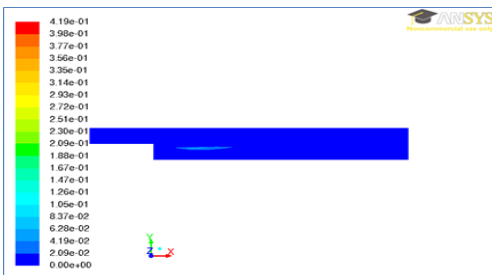


Fig. 4.7 Contours of Rate of Reaction-2

Three points S1, S2, S3 were chosen (co-ordinates as shown in table 4.1). X & Y velocity Frequency was plotted against the amplitude for these points as shown in the figures below.

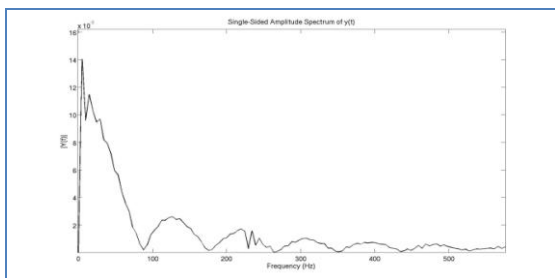


Fig. 4.8 X-velocity frequency for point S1

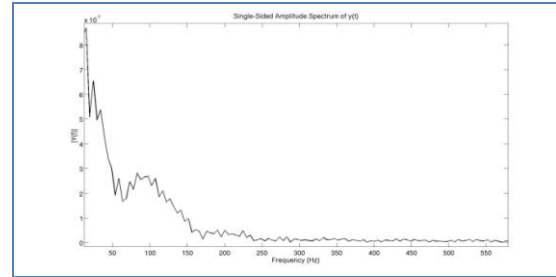


Fig. 4.9 X-velocity frequency for point S2

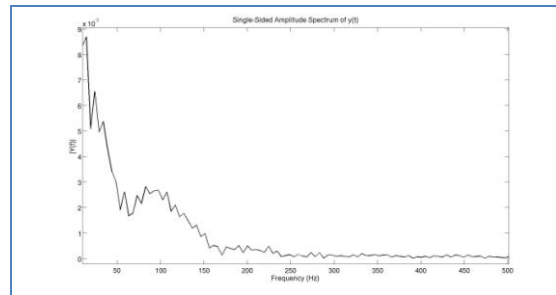


Fig. 4.10 X-velocity frequencies for point S3

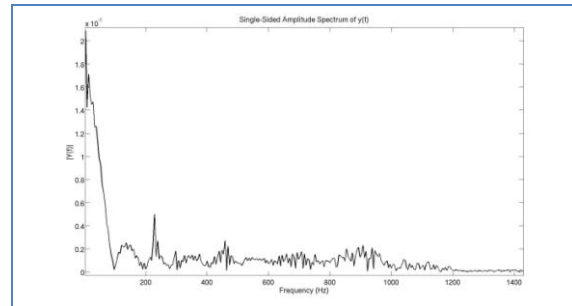


Fig. 4.11 Y-velocity frequency for point S1

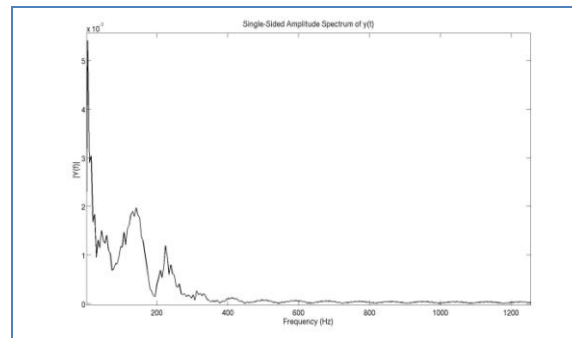


Fig. 4.12 Y-velocity frequency for point S2

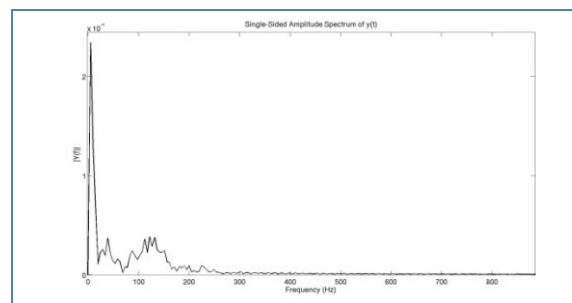


Fig. 4.13 Y-velocity frequency for point S3

points	Location (m)		Amplitude (m)		Frequency (Hz)	
	X coordinate	Y coordinate	X velocity	Y velocity	X velocity	Y velocity
S1	0.01	-0.002	14×10^{-3}	2.2×10^{-3}	12	1
S2	0.1	-0.01	8.5×10^{-3}	5.5×10^{-3}	5	1
S3	0.25	-0.0295	8.5×10^{-3}	2.5×10^{-3}	5	3

Table: 4.1 Amplitude and Frequency

A low-frequency, high amplitude instability was triggered as the magnitude of longitudinal acoustic disturbances. It was observed that as a large vortex was released from the region behind the step, the flame started flapping and caused these low-frequency oscillations. The Strouhal number is defined as $St = fh/U$, where U is the spatio-temporal mean air-flow velocity at the inlet. A constant value of the Strouhal number would indicate that the observed dominant frequency corresponds to that due to any vortex shedding process or shear layer oscillation in the flow field, referred to a vortex shedding mode.

$$St = \frac{fh}{U}$$

Where h is step height i.e. **0.03m**,

f is frequency and

U is spatio-temporal mean air-flow velocity at inlet i.e., **9.42 m/s**

Experimental value for Strouhal number is ≈ 0.02

Strouhal number is calculated for all the three points S1, S2 and S3.

X-velocity frequency	Strouhal Number (St)	Y-velocity frequency	Strouhal Number (St _h)
12 Hz	0.038	1 Hz	0.003
5 Hz	0.016	1 Hz	0.003
5 Hz	0.016	3 Hz	0.01

Table: 4.1 Strouhal Number (St)

RMS Velocity was compared with the experimental data at following locations. $x/h=30$, $x/h=60$, $x/h=90$, $x/h=150$.

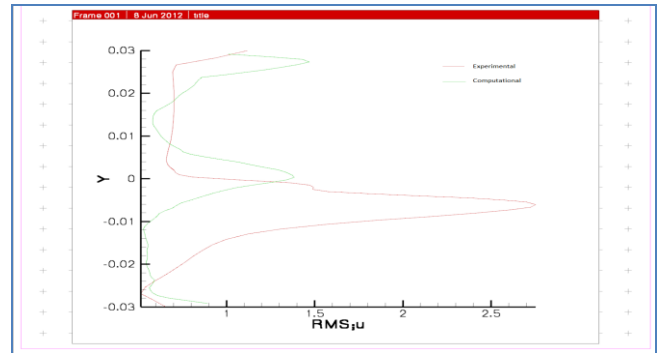


Fig. 4.14 RMS velocity at $x/h=30$

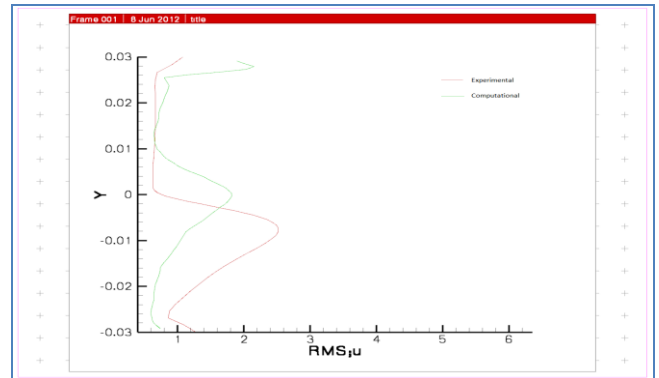


Fig. 4.15 RMS velocity at $x/h=60$

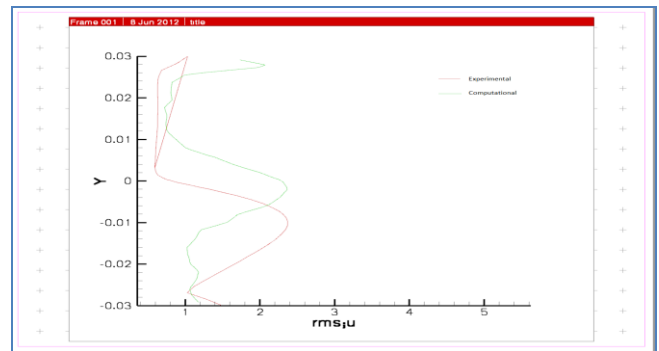


Fig. 4.16 RMS velocity at $x/h=90$

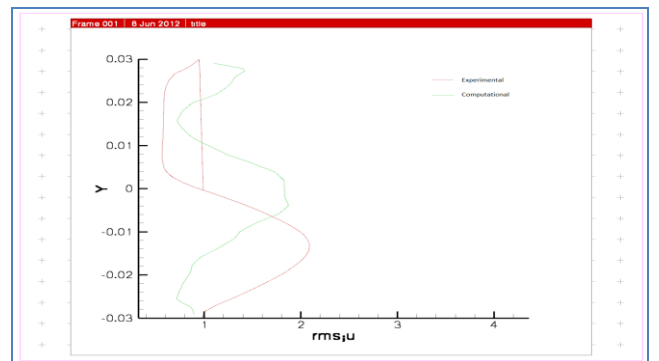


Fig. 4.17 RMS velocity at $x/h=150$

Non dimensional velocity, u/u_{ref} at the location $x/h=6$ was compared with experimental data along Y axis.

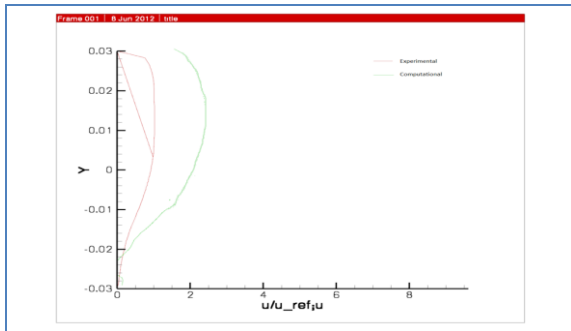


Fig. 4.18 Plot of u/u_{ref} versus Y

Reaction rates were also compared with the existing experimental data. The outline of the flame shown in the image sequence clearly indicates the presence of coherent structures corresponding to large scale vortex roll-up in the shear layer originating from the edge of the backward-facing. Since the images are that of the flame, it follows that the heat release rate fluctuations generating the sound are actually modulated by the vortex shedding process. Further, it can be seen from the image sequence that the fluctuations in the chemiluminescent intensity along with the vortex roll-up and the shedding process is more towards the downstream region of the backward-facing step for this condition.

Experimental Results:

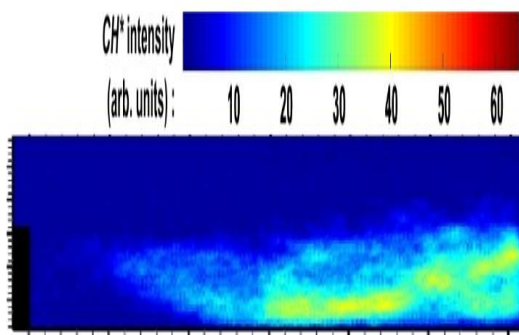


Fig. 4.19 Experimental Results for Heat of Reaction

Computational Results:

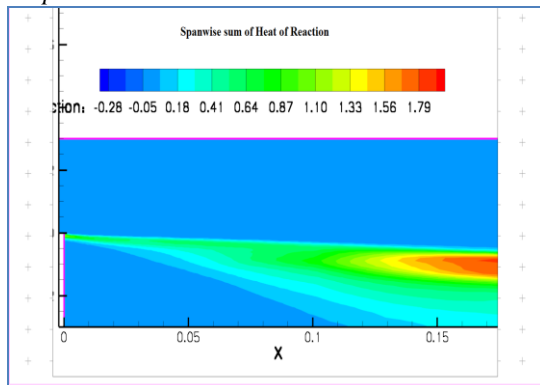


Fig. 4.20 Computational Results for Heat of Reaction

REFERENCES

- 1) Chakravarthy S. R, O. J. Shreenivasan, Benjamin Boehm, Andreas Dreizler and Johannes Janicka (2007) Experimental characterization of onset of acoustic instability in a non-premixed half-dump combustor. *Journal of Acoustical Society of America*, 122 (1), 120–127.
- 2) Chakravarthy S. R, R. Sivakumar and O. J. Shreenivasan (2007) Vortex acoustic lock-on in bluff-body and backward-facing step combustors. *Sadhana*, 32 (parts 1 & 2), 145–154.
- 3) Abu-Mulaweh, H.I., T.S. Chen, and Armaly B.F. (2002), Turbulent mixed convection flow over a backward-facing step the effect of the step heights, *International Journal of Heat and Fluid Flow*, 23, 758-765.
- 4) M.A.Z. Hasan (1991) The flow over a backward-facing step under controlled perturbation: laminar separation
- 5) Chiang, T.P. and T.W.H. Sheu (1999), A numerical revisit of backward facing step flow problem, *Physics of Fluids*, 11, 862-874.
- 6) Cohen, J.M. and T.J. Anderson (2003), Experimental investigation of near blowout instabilities in a lean, premixed step combustor, *AIAA-96-0819*.
- 7) Davis, J.A., N.M. Komerath, R.E. Walterick, W.C. Strahle, and S.G. Lekoudis (1986), Acoustic behavior of an SFRJ simulator, *AIAA-86-0003*.
- 8) Fureby, C. (2000), A computational study of combustion instabilities due to vortex shedding, *Proceedings of the Combustion Institute*, 28, 783-791.
- 9) Ganji, A.J. and R.F. Sawyer (1980), Experimental study of the flow field of a two-dimensional premixed turbulent flame, *AIAA Journal*, 18, No 7, 817-824.
- 10) Hegde, U.G., D. Reuter, and B. T.Zinn (1989), Variable geometry control of reacting shear layers, *AIAA-89-0979*.
- 11) Keller, J.O., L. Vaneveld, D. Korschelt, G.L. Hubbard, A.F. Ghoniem, J.W. Daily and A.K. Oppenheim (1982), Mechanism of instabilities in turbulent combustion leading to flashback, *AIAA Journal*, 20, No. 2, 254-262.
- 12) Langhorne, P.J. (1988), Reheat buzz: acoustically coupled combustion instability. Part I. Experiment, *Journal of Fluid Mechanics*, 193, 417-443.
- 13) Lieuwen, T.C. and B.T. Zinn (2000), On the experimental determination of combustion process driving in an unstable combustor, *Combustion Science and Technology*, 157, 111-127.
- 14) Menon, S. (1992), Active combustion control in a ramjet using large eddy simulations, *Combustion Science and Technology*, 84, 51-79.
- 15) Najm, H.N., and A.F. Ghoniem (1994), Coupling between vorticity and pressure oscillations in combustion instability, *Journal of Propulsion and Power*, 10, No. 6, 769-776.
- 16) Renard, P-H., J.C. Rolon, D.T. Venin, and S. Candel (1999), Investigations of heat release, extinction, and time evolution of the flame surface, for a non-premixed flame interacting with a vortex, *Combustion and Flame*, 117, 189-205.
- 17) Smith, D.A. and E.E. Zukoski (1985), Combustion instability sustained by unsteady vortex combustion, *AIAA-85-1248*.
- 18) Thangam, S. and N. Hur (1991), A highly-resolved numerical study of turbulent separated flow past a backward-facing step, *International Journal of Engineering Science*, 29, 607-615.